ACS APPLIED MATERIALS & INTERFACES

Research Article

www.acsami.org

Performance Enhancement of Quantum-Dot-Sensitized Solar Cells by Potential-Induced Ionic Layer Adsorption and Reaction

I-Ping Liu,[†] Chien-Wei Chang,[†] Hsisheng Teng,[†,‡,§] and Yuh-Lang Lee*[,†,§]

[†]Department of Chemical Engineering, [‡]Center for Micro/Nano Science and Technology, [§]Research Center for Energy Technology and Strategy (RCETS), National Cheng Kung University, Tainan 70101, Taiwan

Supporting Information

ABSTRACT: Successive ionic layer adsorption and reaction (SILAR) technique has been commonly adopted to fabricate quantum-dot-sensitized solar cells (QDSSCs) in the literature. However, pore blocking and poor distribution of quantum dots (QDs) in TiO_2 matrices were always encountered. Herein, we report an efficient method, termed as potential-induced ionic layer adsorption and reaction (PILAR), for in situ synthesizing and assembling CdSe QDs into mesoporous TiO_2 films. In the ion adsorption stage of this process, a negative bias was applied on the TiO_2 film to induce the adsorption of precursor ions. The experimental results show that this bias greatly enhanced the ion adsorption, accumulating a large amount of cadmium ions on the film surface for the following reaction with selenide precursors. Furthermore, this bias also drove cations deep into the bottom region of a TiO_2 film. These effects not only resulted in a higher deposited amount of CdSe, but also a more uniform distribution of the QDs along the TiO_2 film. By using the PILAR process, as well as the SILAR process to replenish the incorporated CdSe, an energy conversion efficiency of 4.30% can be achieved by the CdSe-sensitized solar cell. This performance is much higher than that of a cell prepared by the traditional SILAR process.

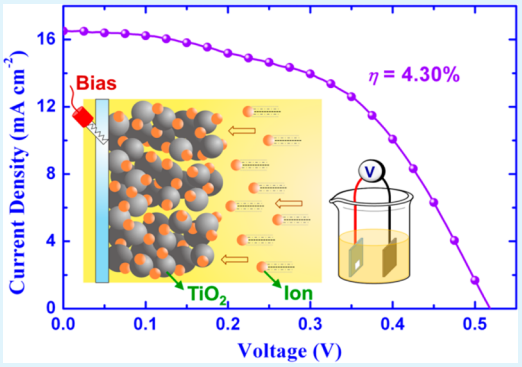

KEYWORDS: *potential-induced assembly, cadmium selenide, quantum-dot-sensitized solar cell, QD distribution, successive ionic layer adsorption and reaction*

1. INTRODUCTION

Dye-sensitized solar cells (DSSCs)[1−3] have attracted increasing interest and are considered to be a potential alternative to silicon-based photovoltaic devices. DSSCs are operated based on photosensitization of mesoporous TiO_2 films using organic sensitizers, and therefore, the performance of DSSCs are intimately controlled by the sensitizer anchored on the TiO_2 surface. Recently, by utilizing a ruthenium complex and zinc porphyrin-based dye as the photoactive sensitizers, energy conversion efficiencies of 11.7[4] and 13.0%[5] have been achieved, respectively.

In addition to the molecular sensitizers commonly used for DSSCs, small band gap semiconductors, such as CdS,[6−8] CdSe,[9−11] PbS,[12−14] and $CuInS_2$,[15−17] have been employed as light harvesters for DSSCs. The advantages of the inorganic semiconductors over dyes include a higher extinction coefficient and greater stability. When the sizes of semiconductors are decreased to the quantum-dot level, these cells are termed as quantum-dot-sensitized solar cells (QDSSCs).[18] Owing to the impact ionization caused by the quantum confinement effect, it is possible for quantum dots (QDs) to generate multiple charge carriers with a single photon excitation.[19,20] Consequently, the theoretical power conversion efficiency of QDSSCs is much higher than that obtained by DSSCs.[21]

Despite the specific advantages of inorganic QDs over molecular dyes, the development of QDSSCs progresses much slower in comparison with that of DSSCs. To date, the state-of-the-art power conversion efficiencies of QDSSCs, ca. 6−7%,[22−24] still lag considerably behind those of DSSCs. The problems encountered in the fabrication of QDSSCs are not only in the development of panchromatic QD sensitizers for expanding the light-harvesting range, but also in the development of suitable electrolytes and counter electrodes for facilitating long-term photostability. Furthermore, assembling QDs into mesoporous TiO_2 matrices is another key that might determine the photovoltaic performance of QDSSCs dramatically.

Two common methods, chemical bath deposition (CBD) and successive ionic layer adsorption and reaction (SILAR), have been adopted to assemble QDs into mesoporous TiO_2 films in many studies reported so far.[25,26] CBD synthesizes colloidal QDs first and then connects the QDs to the TiO_2 surface through a bifunctional linker molecule.[27,28] SILAR, probably the most conventional method, has been employed to in situ synthesize and assemble QDs directly inside TiO_2

Received: August 14, 2014
Accepted: October 21, 2014
Published: October 21, 2014

matrices.[29,30] In the SILAR process, one kind of precursor ion is first adsorbed on the TiO_2 surface and then reacts with other precursor ions to form/deposit QD sensitizers. Because the ionic adsorption is performed spontaneously through interaction between the TiO_2 surface and precursor ions (e.g., Cd^{2+} for CdSe), only a small number of ions is adsorbed within one SILAR cycle. Therefore, repeated adsorption−reaction cycles are required to enhance the number of QD sensitizers on the TiO_2 surface. However, this spontaneous process is performed easily in the outer section of TiO_2 films, but fewer ions can diffuse into the interior of the porous matrix. After conducting several SILAR cycles, the inhomogeneous QD deposition throughout the entire TiO_2 film will lead to a porous blocking by overloaded QDs in the outer region and a deficient QD loading on the inner TiO_2 surface. The blocking of mesopores not only hinders further inner QD deposition but also inhibits the electrolyte penetration into the interior of TiO_2 multilayers, which is anticipated to limit the photovoltaic performance of QDSSCs.

It is difficult to fabricate a TiO_2 film with uniform QD distribution throughout the whole porous matrix by only utilizing the conventional SILAR method. In the literature, various methods have been reported to modify the SILAR process either to improve the penetration of precursor ions into the mesoporous structure[31] or to induce the growth of QDs on the TiO_2 surface.[32] These studies demonstrate that the photovoltaic performance of a QDSSC is intimately related to the coverage and the distribution of QD sensitizers, which are tightly controlled by the QD assembling process.

Application of electrochemistry has been adopted to fabricate QD-sensitized photoelectrodes in some published works.[33−35] In this study, we propose a new process, potential-induced ionic layer adsorption and reaction (denoted as PILAR), for efficient deposition of CdSe QD sensitizers in mesoporous TiO_2 films. In the cationic precursor solution, a negative bias was applied on TiO_2 films to form an electric field, thus driving the cations to diffuse/penetrate into the inner surface of TiO_2 matrices. Because of the electrochemical assistance, a great number of cations could be adsorbed and accumulated over the entire TiO_2 films, which not only enhances the amount of QD deposition but also leads to a more uniform distribution of QDs throughout the whole photoelectrode.

2. EXPERIMENTAL SECTION

2.1. Materials. Two kinds of commercial TiO_2 pastes (PST18NR and PST400C) were purchased from CCIC (Catalysts & Chemicals Industries Co., Ltd., Japan). Cadmium nitrate tetrahydrate ($Cd(NO_3)_2{\cdot}4H_2O$, 99%) was obtained from Sigma-Aldrich. Selenium powder (Se, 200 mesh, 99.999%) was purchased from Alfa Aesar. Sodium sulfide nonahydrate ($Na_2S{\cdot}9H_2O$, 98+%) was purchased from Acros Organics. Zinc acetate dehydrate ($Zn(CH_3COO)_2{\cdot}2H_2O$, 99+%) and sulfur powder (S, 99.5+%) were purchased from Riedel-de Haën. Ethanol (99.9%) was obtained from J. T. Baker. All chemicals were used directly as received without further purification.

2.2. Preparation of TiO_2 Thin Film. Fluorine-doped tin oxide coated glass (FTO, TEC 7, 3 mm thick, 10 Ω sq^{-1}) was used as the substrates in this study. A compact layer post-treatment was carried out by immersing the FTO substrate in a 40 mM aqueous $TiCl_4$ solution at 70 °C for 30 min and then rinsing it with deionized (DI) water and ethanol. TiO_2 nanoparticulate electrodes were prepared by successively screen printing an 8.0 ± 0.5 μm thick transparent layer (PST18NR) and a 4.0 ± 0.5 μm thick light-scattering layer (PST400C) over FTO substrates. To avoid the light scattering effect, we used electrodes for the measurements of UV−vis absorption spectra, X-ray diffraction spectra (XRD), and energy-dispersive X-ray spectrometer (EDS) that were composed of only transparent layers. All the screen printed films were then subjected to a programmed sintering process in air atmosphere: 150 °C for 10 min, 325 °C for 5 min, 450 °C for 5 min, and 500 °C for 30 min.

2.3. Potential-Induced Ionic Layer Adsorption and Reaction (PILAR). For the PILAR process proposed in this work, the adsorption of cadmium ion (Cd^{2+}) was performed under an applied bias. In an electrochemical cell containing 0.1 M $Cd(NO_3)_2$ ethanol electrolyte, a mesoporous TiO_2 electrode and a platinum foil were employed, respectively, as the working and counter electrodes. For each TiO_2 electrode, an electrochemical treatment with 5 successively negative/positive bias steps (e.g., −2.0, +2.0, −2.0, +2.0, and −2.0 V; 60 s for each step) was applied by a CH Instruments potentiostat (CHI627D, Austin, TX) so that the electric field between two electrodes could facilitate the penetration or relaxation of Cd^{2+} in TiO_2 nanoparticulate matrices. A negative bias (e.g., −2.0 V) could induce Cd^{2+} diffusing into the interior of mesopores and accumulating on the inner TiO_2 surface. To avoid the multilayer accumulation, however, a positive bias (e.g., +2.0 V) was also applied to relax the adsorbed ions, leading to a more uniform distribution throughout the entire electrode. After the electrochemical process, the treated electrode was rinsed with ethanol, dried by an air gun, and immersed into the ethanol/water solution (3/7 by volume) containing 0.03 M Na_2SeSO_3 at 50 °C for 5−35 min. The Na_2SeSO_3 solution was prepared according to our previous report.[32] The CdSe-sensitized TiO_2 photoelectrodes prepared by the PILAR process are denoted as TiO_2/*P*-CdSe for the following paragraphs.

2.4. SILAR for CdSe QD Sensitization and ZnS Layers. Conventional SILAR process is also utilized to deposit CdSe QDs for comparison with that by the PILAR method. In brief, a complete SILAR cycle consisted of immersing the electrode successively in two different solutions: one containing 0.05 M $Cd(NO_3)_2$ in ethanol at room temperature as the cation precursor and the other containing 0.03 M Na_2SeSO_3 in the ethanol/DI water solution (3/7 by volume) at 50 °C as the anion precursor. The dipping time in the cation/anion precursor is 5/15 min for the pristine TiO_2 films but 1/1 min for the PILAR treated electrodes. Following each immersion, rinsing and drying was undertaken using ethanol and an air gun, respectively. After the QD sensitization, all electrodes fabricated in this study were coated with ZnS passivation layers by twice dipping alternately into 0.1 M $Zn(CH_3COO)_2$ and 0.1 M Na_2S aqueous solutions for 1 min/dip; the electrodes were rinsed with DI water between dips.

2.5. Device Fabrication. CuS-coated FTO substrates, prepared by the successive ionic solution coating and reaction deposition described in a previous work,[36] were used as the counter electrodes to assemble CdSe-sensitized solar cells. The composition of the polysulfide electrolyte solution was 1.0 M Na_2S, 1.0 M S, and 0.1 M NaOH in DI water. The solar cells were constructed by assembling the CuS counter electrode and CdSe-sensitized electrode with a binder clip separated by a sealing spacer (60 μm thickness, Metlonix 1170−60, Solaronix SA). Then, a polysulfide electrolyte was injected into the cell through the drilled holes on the counter electrode. The active area of the solar cell device analyzed in this study was 0.16 cm^2. In this study, at least two cells were prepared at each condition to verify the reproducibility of cell performance.

2.6. Characterization. UV−vis absorption spectra were recorded with a UV−vis spectrometer constructed by GBC Scientific Equipment (Cintra 10e, Australia). The photovoltaic performance (*J*−*V* curves) of the QDSSCs was evaluated using a digital source meter (6240A, computer-controlled, ADCMT, Japan) with the QDSSC device under standard one sun irradiation (AM 1.5G, 100 mW cm^{-2}) from a solar simulator (XES-301S, class AAA, SAN-EI, Japan) calibrated with a standard silicon reference cell (VS0831, IVT Solar Pte Ltd., Singapore). The incident photon to current efficiency (IPCE) curve was measured by the DC mode method, using an IPCE analyzer (QE-R3011, Enlitech, Taiwan). Electrochemical impedance spectroscopy (EIS) measurements were carried out with the use of a frequency response analyzer (FRA)-equipped potentiostat (PGSTAT30, Autolab) under dark conditions at different forward biases, applying a 10 mV AC sinusoidal signal over the constant applied bias with the

frequency ranging between 100 kHz and 0.01 Hz. Scanning electron microscopic (SEM) images were obtained from the SU8010 (HITACHI, Japan) equipped with an EDS. X-ray photoelectron spectrum were accumulated on an X-ray photoelectron spectroscope (XPS, PHI 5000 VersaProbe, Japan) with Al Kα radiation, and the binding energy was calibrated against the carbon 1s peak set at 284.8 eV. The crystal structures of CdSe QD-sensitized TiO_2 films were characterized by a multipurpose XRD system (Ultima IV, Rigaku, Japan) with Cu Kα radiation excited at 40 kV and 40 mA.

3. RESULTS AND DISCUSSION

To evaluate the effect of an applied potential on the adsorption of cadmium ions (Cd^{2+}), we analyzed the TiO_2 films by X-ray photoelectron spectroscopy (XPS) after executing the ionic adsorption. The results, as shown in Figure 1, demonstrate that

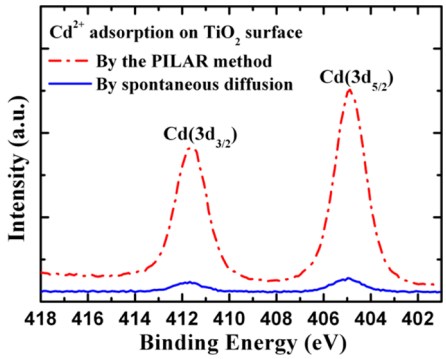

Figure 1. XPS spectra of Cd^{2+}-adsorbed TiO_2 films prepared by spontaneous diffusion and the PILAR method with ±2.0 V.

the Cd(3d) peaks, from the film prepared by spontaneous diffusion/adsorption, show slight intensities, indicating that only a small amount of Cd^{2+} was adsorbed. However, based on the higher intensities of Cd(3d) peaks, an obvious increase in the Cd^{2+} could be detected from the film prepared by the PILAR method with ±2.0 V, which suggests that an applied bias would provide assistance for the adsorption of Cd^{2+}. Besides, the XPS peaks, shown at the identical binding energies for the two films, imply that the applied bias (e.g., ± 2.0 V) for ionic adsorption did not alter the chemical state of the adsorbed Cd^{2+}. Because no plating of cadmium metal was observed, it is inferred that the electrochemical potential utilized in the PILAR method was deemed to facilitate the Cd^{2+} diffusing/transporting in the mesoporous structure, further adsorbing on the TiO_2 surface. Yet, a larger potential would lead to a different situation. As the applied bias increased (e.g., ± 3.0 V), the binding energy of Cd(3d) peaks shifted, and a significant deposition could be observed on the TiO_2 film (possibly the cadmium metal), which suggests that a reduced reaction of cadmium ions might occur owing to the higher electrochemical potential (Figures S1 and S2, Supporting Information). After Cd^{2+} adsorption, the TiO_2 films were immersed into anion precursors at 50 °C (i.e., $SeSO_3^{2-}$) to generate CdSe QD sensitizers in the TiO_2 matrices. As exhibited in Figure S3 (Supporting Information), the color of the PILAR treated CdSe film was obviously lighter for the one prepared by ±1.0 V than the one prepared by ±2.0 V, implying a smaller amount of deposited CdSe QDs. This result also suggests that a higher electrochemical potential is required to facilitate the Cd^{2+} accumulation over the entire TiO_2 film (not exceeding ±2.0 V). On the basis of the analyses mentioned above, we therefore performed the following PILAR experiments with only ±2.0 V.

Figure 2 demonstrates the UV−vis absorption spectra of PILAR treated TiO_2 films with different anionic reaction times.

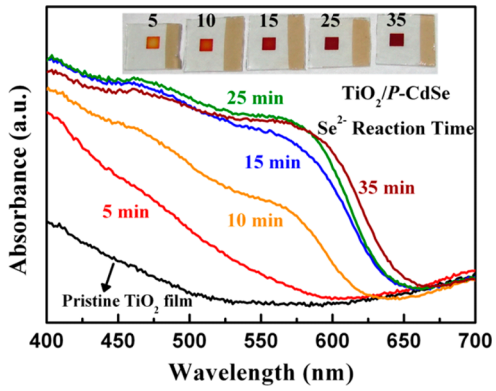

Figure 2. UV−vis absorption spectra of PILAR treated TiO_2 films with various anionic reaction times. (Inset) Photograph of the corresponding CdSe QD-sensitized photoelectrodes.

Compared with the pristine TiO_2 film, the formation of CdSe QDs and their growth behavior could be clearly observed. The absorbance and curve onset edge were enhanced and extended with the increase in reaction time, suggesting an improved deposition of CdSe QDs and a larger particulate size. The inset of Figure 2 displays the color change of different TiO_2 films, from light brown to dark brown, as the anion reaction performed longer. In addition, it shows that the absorbance and the color change of TiO_2 electrodes vary sharply in the early reaction period but become slow after immersion for 15 min. This indicates that most Cd^{2+} adsorbed on TiO_2 surface reacted with anion precursors in 15 min, and the remaining Cd^{2+} might transform completely through longer anion reaction. The above TiO_2 films were further deposited with two ZnS layers by the SILAR technique and then were introduced to assemble QDSSCs. Table 1 summarizes the photovoltaic characteristics

Table 1. Photovoltaic Characteristics for PILAR-Treated CdSe QDSSCs with Various Anionic Reaction Times

Se^{2-} reaction time	J_{sc} (mA cm^{-2})	V_{oc} (mV)	FF	η (%)
5 min	10.50	534	0.49	2.75
10 min	12.33	523	0.47	3.05
15 min	13.52	528	0.47	3.37
25 min	13.64	521	0.48	3.42
35 min	13.03	513	0.51	3.39

of QDSSCs prepared by the corresponding PILAR-treated TiO_2 films. An energy conversion efficiency (η) of 2.75% was achieved for the QDSSC assembled by the film reacting for 5 min, which explains that the PILAR method could effectively facilitate the adsorption of Cd^{2+} in TiO_2 films. Furthermore, the short-circuit photocurrent densities (J_{sc}) and the conversion efficiencies were enhanced with the increase in the anionic reaction time up to 25 min, attributed to the improved light harvesting properties measured from UV−vis spectra mentioned above. For the CdSe QDSSC prepared by the PILAR method and 25 min anion reaction, a conversion efficiency of 3.42% could be obtained. There was no obvious enhancement in photovoltaic performance for an anion reaction longer than 25 min, possibly due to the depletion of adsorbed Cd^{2+} and the desorption of QDs from the TiO_2 surface.

For comparison with the CdSe-sensitized electrode prepared by the PILAR method, the conventional SILAR technique was also employed to synthesize CdSe QDs in a TiO_2 nanoparticulate structure. Figure 3 shows the effect of various SILAR

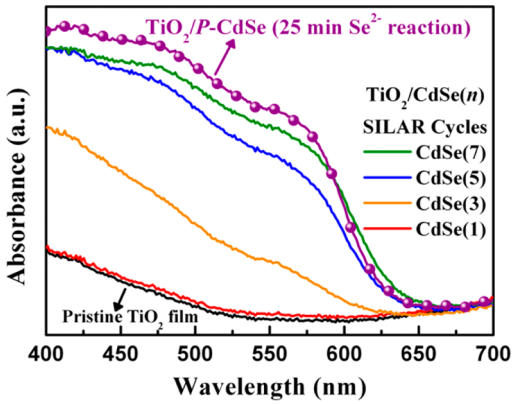

Figure 3. UV–vis absorption spectra of TiO_2 films sensitized by various conventional CdSe SILAR cycles (n). The spectrum of a PILAR-modified film is also plotted for comparison.

cycles on the UV–vis light absorption of CdSe-sensitized films. Apparently, more SILAR cycles would lead to greater absorption intensity and a broader light harvesting region. This means that not only was the number of CdSe QD sensitizers enhanced, but also the effective band gap of the deposited QD was narrowed by increasing SILAR cycles. Moreover, the spectrum of CdSe(1) is very close to that of the pristine TiO_2 film, which demonstrates that only a small amount of Cd^{2+} could be adsorbed on the TiO_2 surface by spontaneous diffusion/adsorption. However, as the SILAR cycle was increased, ions were adsorbed on the QDs anchored on the TiO_2, thus accelerating further QD deposition. In addition, it is noteworthy that the absorbance of CdSe(7) is still lower than that prepared by the PILAR method (25 min anion reaction). The photovoltaic characteristics of CdSe QDSSCs fabricated by the conventional SILAR process are summarized in Table 2. The conversion efficiency for CdSe(1) was only

Table 2. Photovoltaic Characteristics for CdSe QDSSCs Prepared by Various Common SILAR Cycles (n)

SILAR cycle (n)	J_{sc} (mA cm^{-2})	V_{oc} (mV)	FF	η (%)
CdSe(1)	1.53	362	0.40	0.22
CdSe(3)	6.81	473	0.47	1.53
CdSe(5)	8.53	495	0.45	1.91
CdSe(7)	10.03	519	0.49	2.53
CdSe(8)	9.24	525	0.51	2.48

0.3%, but significant enhancements in J_{sc} values, open-circuit photovoltage (V_{oc}), fill factor (FF), and conversion efficiencies (η) could be measured with the increasing SILAR cycles up to 7, which is in agreement with the UV–vis absorption results. The enhanced FF and V_{oc} values also imply a suppressed charge recombination due to the higher coverage of QDs on the TiO_2 surface. As the SILAR cycle was higher than 7, the J_{sc} value and the efficiency decreased dramatically, possibly ascribed to the blocking of outer mesopores by the overloaded QDs. The best conversion efficiency achieved for the CdSe cell prepared by the common SILAR process is 2.53%, which is much lower than that of the PILAR treated device described above (3.42%).

In Figure 3, the light absorption of *P*-CdSe is slightly greater than that of the CdSe(7), which must be one of the causes for the superior photocurrent of the PILAR treated device. However, we believe that there is another reason leading to these results: the coverage or distribution of CdSe QDs in TiO_2 films

To further investigate the influence of the two methods on the cell performance mentioned above, an EDS incorporated in the SEM was utilized to determine the elemental composition of CdSe-sensitized films. At least five positions were measured for each specific depth, and the mean values of the Cd to Ti atomic ratio (Cd/Ti) were calculated, as exhibited in Figure 4.

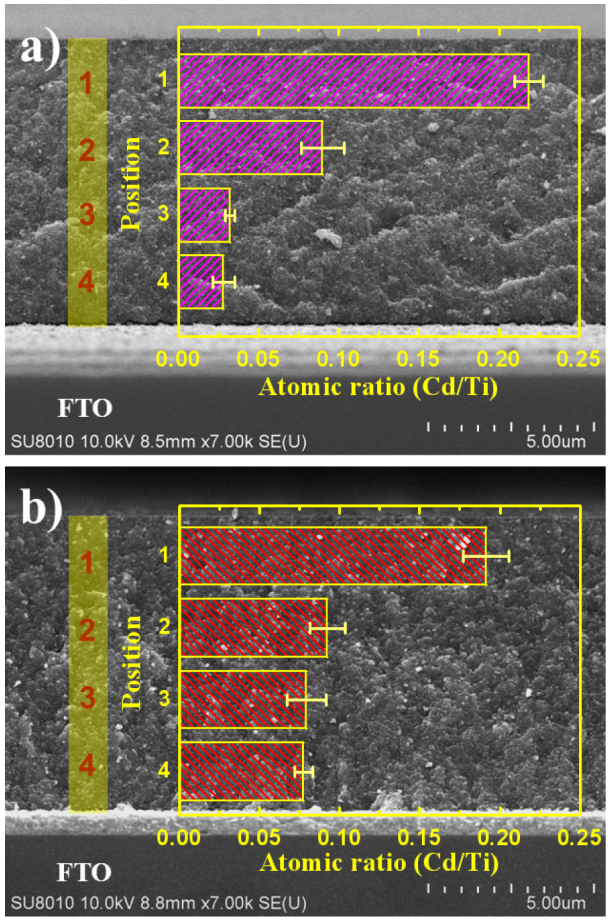

Figure 4. Cross-sectional SEM images and EDS depth profiles of Cd/Ti ratio in the CdSe-sensitized film prepared by (a) the conventional SILAR process with CdSe(7) and (b) the PILAR technique with 25 min anion reaction.

It shows that the Cd/Ti ratios were particularly higher at the outer region of CdSe-sensitized films but decreased gradually with increasing depth, indicating an inhomogeneous QD deposition throughout the entire TiO_2 film. This situation is nearly impossible to avoid, especially for in situ QD growth/assembling techniques adopted in this study. However, compared with the film prepared by the SILAR process in Figure 4a, the Cd/Ti ratios measured at inner positions of the TiO_2 film, (positions 3 and 4) were significantly greater by ca. 2.8 times for that using the PILAR method in Figure 4b. Therefore, based on the above results, it is confirmed that only a small number of ions could diffuse/penetrate spontaneously into the interior of TiO_2 matrices, but a large amount of QD

deposition could accumulate at the outer mesopores. On the contrary, by introducing a driving force from the applied bias (i.e., PILAR), cations could be more favorable to adsorption on the inner TiO_2 surface, thus creating a more uniform distribution and a higher surface coverage of QD sensitizer for TiO_2 films. In addition, the X-ray diffraction spectra (XRD) were measured to identify the CdSe QDs prepared by the two methods. As shown in Figure S4 (Supporting Information), the three spectra (from FTO/TiO_2/*P*-CdSe, FTO/TiO_2/CdSe(7), and FTO/TiO_2) were very similar, and the observed peaks were mainly attributed to the TiO_2 or FTO substrate. However, a weak peak corresponding to the CdSe (2θ = 42.9°) could be identified in the spectra of TiO_2/*P*-CdSe and TiO_2/CdSe(7) films. Therefore, the XRD results confirmed the formation of CdSe QDs in the TiO_2 mesoporous structure.

To unveil the charge transfer behaviors, we characterized the QDSSCs of 25 min and CdSe(7) (Tables 1 and 2, respectively) by electrochemical impedance spectroscopy (EIS) with an equivalent circuit model reported in the literature.[25] The calculation of V_F was applied to relax the voltage drop effect according to the study from the Bisquert group.[37] The charge recombination resistance (R_{rec}) at the photoelectrode/electrolyte interface, and the electron lifetime as a function of V_F are plotted in Figure 5, panels a and b, respectively. Apparently, a

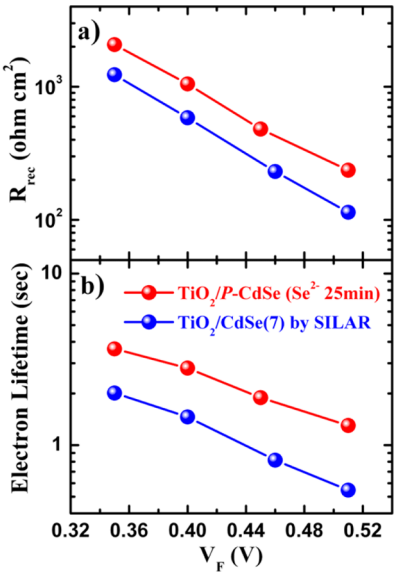

Figure 5. Impedance characterization of QDSSCs prepared by different techniques: (a) charge recombination resistance and (b) electron lifetime as a function of V_F.

larger R_{rec} and longer electron time could be obtained in the PILAR treated QDSSC, meaning a suppressed charge recombination at the electrode/electrolyte interface. These results not only were attributed to the improved surface coverage and more uniform distribution of CdSe QDs, but also were in good agreement with the superior photovoltaic performance of the cell device.

On the basis of the results exhibited above, we could conclude that, compared with the conventional SILAR process, the PILAR method proposed in this study for CdSe QD deposition is beneficial in assembling highly efficient QDSSCs due to its simplicity, time-saving properties, and enhanced QD loading with superior distribution. A schematic diagram was drawn to illustrate the distribution of QDs in TiO_2 films, as shown in Figure 6. For the electrode prepared by the common SILAR process, because of the slight QD deposition in the

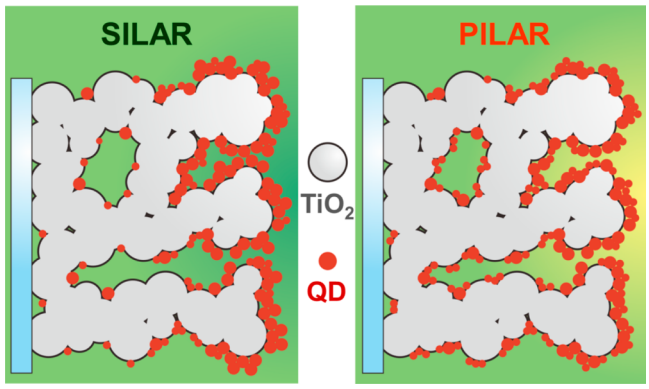

Figure 6. Schematic diagram of the CdSe-sensitized photoelectrode prepared by utilizing different QD assembling techniques.

interior of the nanoparticulate structure, the coverage of QDs on the TiO_2 surface is usually incomplete. The naked TiO_2 surface would become the position where the interfacial recombination happens, lowering the electron lifetime as well as the conversion efficiency of the device. On the other hand, the electrode sensitized QDs by the PILAR method reveal abundant QD deposition with an improved distribution/coverage at the inner region of TiO_2 films. Consequently, the excited photoelectron has much less opportunity to recombine with polysulfide electrolytes, and thus, better photovoltaic performance could be obtained.

To further improve the conversion efficiency, we adopted a strategy of combining the PILAR and SILAR processes to prepare CdSe-sensitized films. Briefly, the pristine TiO_2 film first carried out the PILAR method incorporating a 25 min anion reaction, and then, the conventional SILAR process was employed for further QD deposition. Because a significant amount of QDs had been already deposited by the PILAR process, a short dipping time (1/1 min in cation/anion precursor) was employed in the SILAR process to achieve a low QD deposition rate, avoiding the blocking of mesopores. Figure 7a demonstrates the effect of additional SILAR cycles on the UV−vis absorption spectra of PILAR modified films. As the SILAR cycle increased, the light absorption was clearly enhanced, and the curve onsets were extended to a longer wavelength region, as well. This indicates that after conducting the PILAR method, there was still room for the formation and growth of QD sensitizers in TiO_2 films. The *J*−*V* characteristics of QDSSCs employing PILAR and SILAR processes are presented in Figure 7b, and the corresponding photovoltaic parameters are summarized in Table 3. Increasing SILAR cycles could lead to an enhanced J_{sc} value and improve conversion efficiency (<10 cycles), which matches well with the tendency of light absorption in Figure 7a for an enhanced QD deposition. However, when performing the SILAR process for more than 10 cycles, like the device *P*-CdSe/CdSe(12) shown in Table 3, the cell performance decreased even though a higher amount of QDs was deposited, which could be ascribed to the mesoporous blocking by overloaded QDs. The present results demonstrated that by introducing the additional QD loading of 10 SILAR cycles, the energy conversion efficiency could be boosted further from 3.42 to 4.30%. As shown in the inset in Figure 7b, the incident photon to current efficiency spectrum

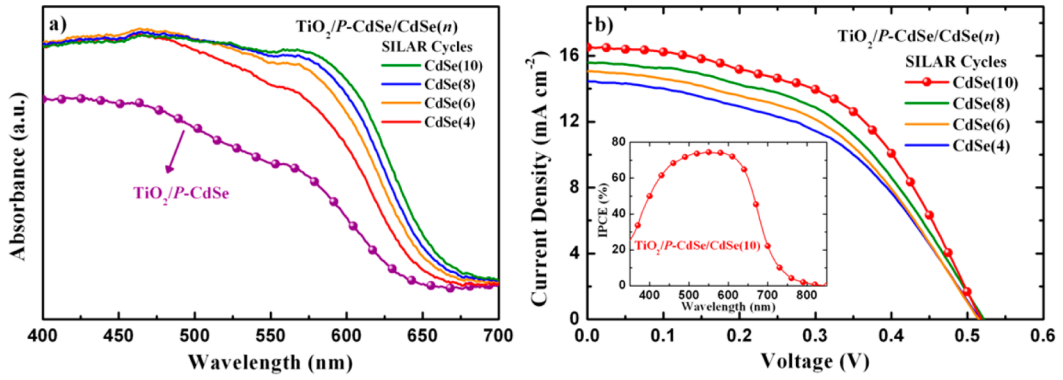

Figure 7. (a) UV–vis absorption spectra of PILAR treated TiO_2 films with various CdSe SILAR cycles (n). The spectrum of a film without the SILAR deposition is also plotted for comparison. (b) J–V characteristics of CdSe QDSSCs prepared by the PILAR and various SILAR cycles (n). (Inset) IPCE spectrum of the P-CdSe/CdSe(10) device.

Table 3. Photovoltaic Parameters of CdSe QDSSCs Prepared by the Combination of the PILAR and Various SILAR Cycles (n)

SILAR cycle (n)	J_{sc} (mA cm^{-2})	V_{oc} (mV)	FF	η (%)
P-CdSe/CdSe(4)	14.16	517	0.47	3.54
P-CdSe/CdSe(6)	15.06	517	0.48	3.71
P-CdSe/CdSe(8)	15.59	515	0.49	3.95
P-CdSe/CdSe(10)	16.50	514	0.51	4.30
P-CdSe/CdSe(12)	10.29	489	0.45	2.29

(IPCE) of the P-CdSe/CdSe(10) cell is nearly consistent with the light absorption properties of the corresponding photoelectrode.

To summarize, the most significant advantages of the PILAR method for assembling QD sensitizers in TiO_2 films are not only the enhanced QD deposition, but also the simultaneously improved QD distribution/coverage throughout the entire films. Owing to the unavoidably poor QD distribution resulting from the conventional SILAR process, the PILAR method allows cations to diffuse into the interior of TiO_2 matrices, which is anticipated to achieve an inferior charge recombination and higher energy conversion efficiency for a QDSSC. Combination of the PILAR and SILAR processes could offer the opportunity to further increase the photovoltaic performance by more QD loading and improved light harvesting capability. Until now, efforts have been underway to study the application of the PILAR method on other anion precursors[29] or different QD systems, for example, CdS, $CuInS_2$, and CdS/CdSe with a cascade architecture.[38,39] Better photovoltaic performance are expected to be achieved.

4. CONCLUSIONS

In conclusion, a simple and time-saving method, PILAR, was developed for efficient CdSe QDSSC fabrication by introducing an electric field to facilitate cations diffusion into the interior of TiO_2 multilayers. Experimental results demonstrated that a significant enhancement of QD loading was achieved by adopting the PILAR approach. Furthermore, in comparison with the film prepared by the conventional SILAR technique, the QD distribution throughout the entire TiO_2 matrices and the coverage on the TiO_2 surface were unexpectedly improved in the PILAR treated films. Based on the suppressed charge recombination attributable to the superior QD distribution, a high conversion efficiency of 3.42% was measured in the QDSSC using only the PILAR method with a 25 min anion reaction. Moreover, with the addition of the SILAR process to allow further QD deposition, the energy conversion efficiency could be increased up to 4.30% under full sun illumination. We believe that the PILAR method proposed in this study provides an easy and promising route for QDSSC fabrication, and the exploration for different QD sensitization is currently in progress.

■ ASSOCIATED CONTENT

Supporting Information

XPS spectra and SEM images of TiO_2 films prepared by the PILAR method with ±2.0 and ±3.0 V applied biases. This material is available free of charge via the Internet at http://pubs.acs.org.

■ AUTHOR INFORMATION

Corresponding Author

*E-mail: yllee@mail.ncku.edu.tw. Tel: +886-6-2757575 ext. 62693. Fax: +886-6-2344496.

Notes

The authors declare no competing financial interest.

■ ACKNOWLEDGMENTS

The authors appreciate research funding from the Ministry of Science and Technology (MOST) of Taiwan (NSC 103-ET-E-006-008-ET, MOST 103-2622-E-006-010-CC2, and 103-2221-E-006-248-MY3) and financial support from the Headquarters of University Advancement at the National Cheng Kung University, which is sponsored by the Ministry of Education, Taiwan, ROC. We acknowledge Prof. Jrjeng Ruan for assistance with XRD measurement and Dr. Ching-Fa Chi for fruitful discussions and helpful suggestions.

■ REFERENCES

(1) Grätzel, M. Photoelectrochemical Cells. *Nature* **2001**, *414*, 338–344.
(2) Grätzel, M. Solar Energy Conversion by Dye-Sensitized Photovoltaic Cells. *Inorg. Chem.* **2005**, *44*, 6841–6851.
(3) Hagfeldt, A.; Boschloo, G.; Sun, L.; Kloo, L.; Pettersson, H. Dye-Sensitized Solar Cells. *Chem. Rev.* **2010**, *110*, 6595–6663.
(4) Yu, Q.; Wang, Y.; Yi, Z.; Zu, N.; Zhang, J.; Zhang, M.; Wang, P. High-Efficiency Dye-Sensitized Solar Cells: The Influence of Lithium Ions on Exciton Dissociation, Charge Recombination, and Surface States. *ACS Nano* **2010**, *4*, 6032–6038.
(5) Mathew, S.; Yella, A.; Gao, P.; Humphry-Baker, R.; Curchod, B. F. E.; Ashari-Astani, N.; Tavernelli, I.; Rothlisberger, U.; Nazeeruddin,

Md. K.; Grätzel, M. Dye-Sensitized Solar Cells with 13% Efficiency Achieved through the Molecular Engineering of Porphyrin Sensitizers. *Nat. Chem.* **2014**, *6*, 242−247.
(6) Zhu, G.; Pan, L.; Xu, T.; Sun, Z. One-Step Synthesis of CdS Sensitized TiO_2 Photoanodes for Quantum Dot-Sensitized Solar Cells by Microwave Assisted Chemical Bath Deposition Method. *ACS Appl. Mater. Interfaces* **2011**, *3*, 1472−1478.
(7) Yeh, M.-H.; Lin, L.-Y.; Lee, C.-P.; Chou, C.-Y.; Tsai, K.-W.; Lin, J.-T.; Ho, K.-C. High Performance CdS Quantum-Dot-Sensitized Solar Cells with Ti-Based Ceramic Materials as Catalysts on the Counter Electrode. *J. Power Sources* **2008**, *237*, 141−148.
(8) Rabinovich, E.; Hodes, G. Effective Bandgap Lowering of CdS Deposited by Successive Ionic Layer Adsorption and Reaction. *J. Phys. Chem. C* **2013**, *117*, 1611−1620.
(9) Coughlin, K. M.; Nevins, J. S.; Watson, D. F. Aqueous-Phase Linker-Assisted Attachment of Cysteinate(2^-)-Capped CdSe Quantum Dots to TiO_2 for Quantum Dot-Sensitized Solar Cells. *ACS Appl. Mater. Interfaces* **2013**, *5*, 8649−8654.
(10) Liu, F.; Zhu, J.; Wei, J.; Li, Y.; Hu, L.; Huang, Y.; Takuya, O.; Shen, Q.; Toyoda, T.; Zhang, B.; Yao, J.; Dai, S. Ex Situ CdSe Quantum Dot-Sensitized Solar Cells Employing Inorganic Ligand Exchange To Boost Efficiency. *J. Phys. Chem. C* **2014**, *118*, 214−222.
(11) Yun, H. J.; Paik, T.; Edley, M. E.; Baxter, J. B.; Murray, C. B. Enhanced Charge Transfer Kinetics of CdSe Quantum Dot-Sensitized Solar Cell by Inorganic Ligand Exchange Treatments. *ACS Appl. Mater. Interfaces* **2014**, *6*, 3721−3728.
(12) Lee, J.-W.; Son, D.-Y.; Ahn, T. K.; Shin, H.-W.; Kim, I. Y.; Hwang, S.-J.; Ko, M. J.; Sul, S.; Han, H.; Park, N.-G. Quantum-Dot-Sensitized Solar Cell with Unprecedentedly High Photocurrent. *Sci. Rep.* **2013**, *3*, 1050.
(13) González-Pedro, V.; Sima, C.; Marzari, G.; Boix, P. P.; Giménez, S.; Shen, Q.; Dittrich, T.; Mora-Seró, I. High Performance PbS Quantum Dot Sensitized Solar Cells Exceeding 4% Efficiency: The Role of Metal Precursors in the Electron Injection and Charge Separation. *Phys. Chem. Chem. Phys.* **2013**, *15*, 13835−13843.
(14) Sung, S. D.; Lim, I.; Kang, P.; Lee, C.; Lee, W. I. Design and Development of Highly Efficient PbS Quantum Dot-Sensitized Solar Cells Working in an Aqueous Polysulfide Electrolyte. *Chem. Commun.* **2013**, *49*, 6054−6056.
(15) Chang, C.-C.; Chen, J.-K.; Chen, C.-P.; Yang, C.-H.; Chang, J.-Y. Synthesis of Eco-Friendly $CuInS_2$ Quantum Dot-Sensitized Solar Cells by a Combined Ex Situ/in Situ Growth Approach. *ACS Appl. Mater. Interfaces* **2013**, *5*, 11296−11306.
(16) Luo, J.; Wei, H.; Huang, Q.; Hu, X.; Zhao, H.; Yu, R.; Li, D.; Luo, Y.; Meng, Q. Highly Efficient Core−Shell $CuInS_2$−Mn Doped CdS Quantum Dot Sensitized Solar Cells. *Chem. Commun.* **2013**, *49*, 3881−3883.
(17) Chang, J.-Y.; Lin, J.-M.; Su, L.-F.; Chang, C.-F. Improved Performance of $CuInS_2$ Quantum Dot-Sensitized Solar Cells Based on a Multilayered Architecture. *ACS Appl. Mater. Interfaces* **2013**, *5*, 8740−8752.
(18) Kamat, P. V. Quantum Dot Solar Cells. The Next Big Thing in Photovoltaics. *J. Phys. Chem. Lett.* **2013**, *4*, 908−918.
(19) Nozik, A. J. Making the Most of Photons. *Nat. Nanotechnol.* **2009**, *4*, 548−549.
(20) Beard, M. C.; Midgett, A. G.; Hanna, M. C.; Luther, J. M.; Hughes, B. K.; Nozik, A. J. Comparing Multiple Exciton Generation in Quantum Dots To Impact Ionization in Bulk Semiconductors: Implications for Enhancement of Solar Energy Conversion. *Nano Lett.* **2010**, *10*, 3019−3027.
(21) Hanna, M. C.; Nozik, A. J. Solar Conversion Efficiency of Photovoltaic and Photoelectrolysis Cells with Carrier Multiplication Absorbers. *J. Appl. Phys.* **2006**, *100*, 074510.
(22) Pan, Z.; Zhao, K.; Wang, J.; Zhang, H.; Feng, Y.; Zhong, X. Near Infrared Absorption of $CdSe_xTe_{1-x}$ Alloyed Quantum Dot Sensitized Solar Cells with More than 6% Efficiency and High Stability. *ACS Nano* **2013**, *7*, 5215−5222.
(23) Wang, J.; Mora-Seró, I.; Pan, Z.; Zhao, K.; Zhang, H.; Feng, Y.; Yang, G.; Zhong, X.; Bisquert, J. Core/Shell Colloidal Quantum Dot Exciplex States for the Development of Highly Efficient Quantum-Dot-Sensitized Solar Cells. *J. Am. Chem. Soc.* **2013**, *135*, 15913−15922.
(24) Pan, Z.; Mora-Seró, I.; Shen, Q.; Zhang, H.; Li, Y.; Zhao, K.; Wang, J.; Zhong, X.; Bisquert, J. High-Efficiency "Green" Quantum Dot Solar Cells. *J. Am. Chem. Soc.* **2014**, *136*, 9203−9210.
(25) Mora-Seró, I.; Giménez, S.; Fabregat-Santiago, F.; Gómez, R.; Shen, Q.; Toyoda, T.; Bisquert, J. Recombination in Quantum Dot Sensitized Solar Cells. *Acc. Chem. Res.* **2009**, *42*, 1848−1857.
(26) Mora-Seró, I.; Bisquert, J. Breakthroughs in the Development of Semiconductor-Sensitized Solar Cells. *J. Phys. Chem. Lett.* **2010**, *1*, 3046−3052.
(27) Robel, I.; Subramanian, V.; Kuno, M.; Kamat, P. V. Quantum Dot Solar Cells. Harvesting Light Energy with CdSe Nanocrystals Molecularly Linked to Mesoscopic TiO_2 Films. *J. Am. Chem. Soc.* **2006**, *128*, 2385−2393.
(28) Shen, Y.-J.; Lee, Y.-L. Assembly of CdS Quantum Dots onto Mesoscopic TiO_2 Films for Quantum Dot-Sensitized Solar Cell Applications. *Nanotechnology* **2008**, *19*, 045602.
(29) Lee, H.; Wang, M.; Chen, P.; Gamelin, D. R.; Zakeeruddin, S. M.; Grätzel, M.; Nazeeruddin, Md. K. Efficient CdSe Quantum Dot-Sensitized Solar Cells Prepared by an Improved Successive Ionic Layer Adsorption and Reaction Process. *Nano Lett.* **2009**, *9*, 4221−4227.
(30) Becker, M. A.; Radich, J. G.; Bunker, B. A.; Kamat, P. V. How Does a SILAR CdSe Film Grow? Tuning the Deposition Steps to Suppress Interfacial Charge Recombination in Solar Cells. *J. Phys. Chem. Lett.* **2014**, *5*, 1575−1582.
(31) Chang, C.-H.; Lee, Y.-L. Chemical Bath Deposition of CdS Quantum Dots onto Mesoscopic TiO_2 Films for Application in Quantum-Dot-Sensitized Solar Cells. *Appl. Phys. Lett.* **2007**, *91*, 053503.
(32) Chong, L.-W.; Chien, H.-T.; Lee, Y.-L. Assembly of CdSe onto Mesoporous TiO_2 Films Induced by a Self-Assembled Monolayer for Quantum Dot-Sensitized Solar Cell Applications. *J. Power Sources* **2010**, *195*, 5109−5113.
(33) Salant, A.; Shalom, M.; Hod, I.; Faust, A.; Zaban, A.; Banin, U. Quantum Dot Sensitized Solar Cells with Improved Efficiency Prepared Using Electrophoretic Deposition. *ACS Nano* **2010**, *4*, 5962−5968.
(34) Benehkohal, N. P.; González-Pedro, V.; Boix, P. P.; Chavhan, S.; Tena-Zaera, R.; Demopoulos, G. P.; Mora-Seró, I. Colloidal PbS and PbSeS Quantum Dot Sensitized Solar Cells Prepared by Electrophoretic Deposition. *J. Phys. Chem. C* **2012**, *116*, 16391−16397.
(35) Santra, P. K.; Nair, P. V.; Thomas, K. G.; Kamat, P. V. $CuInS_2$-Sensitized Quantum Dot Solar Cell. Electrophoretic Deposition, Excited-State Dynamics, and Photovoltaic Performance. *J. Phys. Chem. Lett.* **2013**, *4*, 722−729.
(36) Li, T.-L.; Lee, Y.-L.; Teng, H. High-Performance Quantum Dot-Sensitized Solar Cells Based on Sensitization with $CuInS_2$ Quantum Dots/CdS Heterostructure. *Energy Environ. Sci.* **2012**, *5*, 5315−5324.
(37) González-Pedro, V.; Xu, X.; Mora-Seró, I.; Bisquert, J. Modeling High-Efficiency Quantum Dot Sensitized Solar Cells. *ACS Nano* **2010**, *4*, 5783−5790.
(38) Lin, K.-H.; Chuang, C.-Y.; Lee, Y.-Y.; Li, F.-C.; Chang, Y.-M.; Liu, I.-P.; Chou, S.-C.; Lee, Y.-L. Charge Transfer in the Heterointerfaces of CdS/CdSe Cosensitized TiO_2 Photoelectrode. *J. Phys. Chem. C* **2012**, *116*, 1550−1555.
(39) Zhu, G.; Pan, L.; Xu, T.; Sun, Z. CdS/CdSe-Cosensitized TiO_2 Photoanode for Quantum-Dot-Sensitized Solar Cells by a Microwave-Assisted Chemical Bath Deposition Method. *ACS Appl. Mater. Interfaces* **2011**, *3*, 3146−3151.